(9) DiAndreth, J. R.; Paulaitis, M. E., *Am. Chem. Soc., Div. Fuel Chem. Prepr. Pap.* **1985**, *30*, 57-61.
(10) Fleck, R. N., Ph.D. Dissertation, University of California, Berkeley, CA, 1967.
(11) Panagiotopoulos, A. Z.; Reid, R. C. *ACS Symp. Ser.* **1987**, *329*, 115-129.
(12) Panagiotopoulos, A. Z.; Reid, R. C. *Fluid Phase Equilib.* **1986**, *29*, 525-534.
(13) Snedeker, R. A. Ph.D. Dissertation, Princeton University, Princeton, NJ, 1955.
(14) Elgin, J. C.; Weinstock, J. J. *J. Chem. Eng. Data* **1959**, *4*, 3-12.
(15) Francis, A. W. *J. Phys. Chem.* **1954**, *58*, 1099-1114.
(16) Shimshick, E. J. *CHEMTECH* **1983**, *13*, 374-375.
(17) Panagiotopoulos, A. Z. Ph.D. Dissertation, Massachusetts Institute of Technology, Cambridge, MA, 1986.
(18) Wiebe, R.; Gaddy, V. L. *J. Am. Chem. Soc.* **1941**, *63*, 475-77.
(19) Wiebe, R. *Chem. Rev.* **1941**, *29*, 475-81.
(20) Katayama, T.; Oghaki, K.; Maekawa, G.; Goto, M.; Nagano, T. *J. Chem. Eng. Jpn* **1975**, *8*, 89-92.
(21) Peng, D-Y.; Robinson, D. B. *Ind. Eng. Chem. Fundam.* **1976**, *15*, 59-64.
(22) Panagiotopoulos, A. Z.; Kumar, S. *Fluid Phase Equilib.* **1985**, *22*, 77-88.
(23) Reid, R. C.; Prausnitz, J. M.; Sherwood, T. K. *The Properties of Gases and Liquids*, 3d ed.; McGraw-Hill: New York, 1977.
(24) Willson, R. C. Ph.D. Dissertation, Massachusetts Institute of Technology, Cambridge, MA, 1988.
(25) Alessi, P.; Kikic, I.; Fermeglia, M. *Fluid Phase Equil.* **1984**, *18*, 93.

Received for review August 3, 1987. Accepted January 22, 1988. Financial support for this work was provided by the National Science Foundation, under Grant CPE-8318494.

Measurement and Model Prediction of Solubilities of Pure Fatty Acids, Pure Triglycerides, and Mixtures of Triglycerides in Supercritical Carbon Dioxide

Thomas Bamberger,[†] John C. Erickson,[*] and Charles L. Cooney
Biochemical Process Engineering Center, Massachusetts Institute of Technology, Cambridge, Massachusetts 02139

Sanat K. Kumar[‡]
Department of Chemical Engineering, Massachusetts Institute of Technology, Cambridge, Massachusetts 02139

The solubilities in CO_2 of three pure triglycerides (trilaurin, trimyristin, and tripalmitin) and their corresponding fatty acids (lauric acid, myristic acid, and palmitic acid) were measured at 313 K and at pressures between 8 and 30 MPa. The data were correlated by using a lattice model equation of state. Solubilities of members of a homologous series (fatty acid or triglyceride) decreased with increasing molecular weight in accordance with previous findings. Solubilities of triglyceride mixtures in CO_2 were also measured. The solubility of the most soluble compound in the mixture was the same as the pure component solubility of that compound, but the solubilities of the less soluble species in mixtures were enhanced by the presence of more soluble triglycerides.

Introduction

Edible oils are normally produced by extracting lipids from biological materials (such as soybeans) using *n*-hexane as a solvent. The high flammability and adverse health affects of residual solvent in food products make hexane a poor choice from an industrial standpoint. Because of these issues, supercritical fluids (SCF), especially supercritical carbon dioxide which is both nontoxic and nonflammable, are now being considered as replacements for hexane (*1*, *2*). SCF extraction of lipids has been studied extensively in recent years (*2*–*15*) and a more comprehensive review has been prepared by McHugh and Krukonis (*1*).

The first reported commercial process using SCF for the fractionation of lipids was the Solexol process developed by the M. W. Kellogg Co. in 1947 (*16*, *17*). Supercritical propane was used to extract and fractionate edible oils in this process. Six plants were built to refine fish oil, animal fat, and vegetable oils (*17*).

More recently, Eisenbach (*7*) has described the separation of eicosapentenoic acid ethyl ester ($C_{20:5}$) from a mixture of fatty acid ethyl esters derived from codfish oil using CO_2 at a constant temperature (323 K) and pressure (15 MPa). All of the fatty acid ethyl esters present in the mixture are soluble in CO_2 to some extent, but at the beginning of the extraction, the lower molecular weight esters are extracted preferentially. After most of the light esters have been stripped away, the desired product is then extracted in fairly high purity. Using a two-step process, Eisenbach achieved a product purity of approximately 92% with a yield of about 80%.

While processes for the fractionation of oils have been tested, not much is known about the physical chemistry of lipid solubility in supercritical fluids. Most of the available information deals with bulk solubilities of complex oils in SCF, with little data on the solubilities of the individual components of these mixtures. The only published quantitative data on the solubilities of pure fatty acids and triglycerides were measured by Chrastil (*5*) who reported the individual CO_2 solubilities of the following lipids: stearic acid, oleic acid, behenic acid, tributyrin, tripalmitin, tristearin, triolein, and trilinolein in the temperature range of 313-353 K and at pressures between 8 and 25 MPa.

In the present work, the solubilities of pure fatty acids and pure triglycerides were measured. The fatty acids used were lauric, myristic, and palmitic acids. The triglycerides were trilaurin (LLL), trimyristin (MMM), and tripalmitin (PPP). A recently developed lattice equation of state (EOS) (*18*) was used successfully to correlate the experimental data by using a single adjustable parameter per binary. The following triglyceride mixtures were also studied: LLL–MMM–CO_2, LLL–PPP–CO_2, MMM–PPP–CO_2, and LLL–MMM–PPP–CO_2. All measurements were made at 313 K and at pressures between 8 and 30 MPa.

---

[*] Author to whom all correspondence should be addressed.
[†] Present address: Institut für Thermische Verfahrenstechnik der Universität Karlsruhe, Kaiserstr. 12, D-7500 Karlsruhe 1, West Germany.
[‡] Present address: IBM Almaden Research Laboratory, Dept K91, 650 Harry Rd. San Jose, CA 95120.

0021-9568/88/1733-0327$01.50/0 © 1988 American Chemical Society

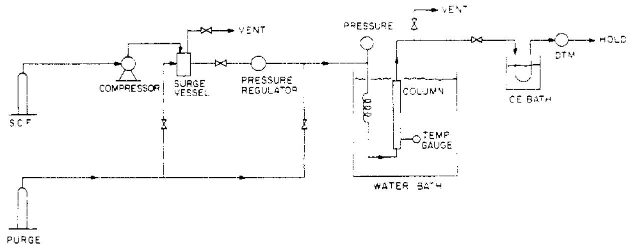

Figure 1. Schematic of experimental apparatus.

Experimental Methods and Materials

Equipment. Solubility measurements were carried out in the high-pressure flow-through apparatus shown in Figure 1. A detailed description of the equipment and the experimental procedure is given elsewhere (*19*, *20*).

The equilibrium cell was a stainless steel column of 30.5 cm length and 1.7 cm inner diameter. It was filled with alternating layers of glass wool and lipid crystals in order to minimize channeling. The equilibrium cell was immersed in a water bath, which was maintained at 313 ± 0.1 K with a temperature regulator (B. Braun). The temperature of the water bath was measured with a mercury thermometer accurate to ±0.1 K and the temperature inside the cell was read by an iron–constantan thermocouple (Omega) to ±0.2 K. The cell was maintained at isobaric conditions, to ±0.1 MPa at pressures above 15 MPa, and ±0.05 MPa at lower pressures, with a pressure regulator (Matheson). A Heise Bourdon gauge measured the pressure inside the cell to within ±0.05 MPa.

Procedure. The supercritical carbon dioxide stream was contacted with the lipids and flashed to atmospheric pressure through a heated pressure reduction valve (Autoclave Engineers), and the precipitated solute was trapped in a cooled U-tube. The weight of solute was determined by weighing the U-tube (and the short stainless steel fitting connecting the U-tube to the flash valve) to ±0.01 mg in a Mettler analytical balance before and after the extracton. The volume of expanded gas was measured by a dry test meter (Singer) to ±10 cm^3.

To examine possible limitations caused by mass transfer, the solubility of naphthalene was determined at 318 K and 11 MPa over a range of CO_2 flow rates from 26 to 45 mg/s. The readings differed from each other by only ±1% and the maximum deviation from literature data (*21*) was 3.5%. Therefore, an intermediate mass flow of about 30 mg/s was used in our experiments. In addition, at the end of each set of experiments, the first run was repeated with a 20% higher mass flow of carbon dioxide. Although in some cases more than 70% of the initial charge of the equilibrium cell was extracted, the readings never differed by more than the uncertainty of the measurement, which was shown by standard error analysis to be never more than ±6%.

Analysis of Mixtures. The U-tube containing the precipitated solute was rinsed with chloroform to dissolve all lipids. Then, 0.5 μL of the resulting solution was injected into an HP 5830A gas chromatograph equipped with a capillary column and on-column injector. The column was a 10 m × 0.53 mm fused silica open tubular (FSOT) column coated with 1-μm poly(phenylmethylsiloxane) (RSL-300 from Alltech-Applied Science). Hydrogen was the carrier gas, the column inlet pressure was 10 kPa, and the oven temperature was programmed from 553 to 613 K. The chromatographic response factors were determined by analyzing standard mixtures prepared gravimetrically. Periodic injections of standard mixtures produced reproducible peak areas on the GC. The uncertainty never exceeded ±3%.

The composition inside the equilibrium cell was calculated based on a mass balance between the initial mass of lipid loaded in the cell and the mass extracted during the previous experiments.

Melting Point Depression. One-tenth of a gram of a pure lipid or of a lipid mixture (of approximately the same composition as that used for the solubility experiments) was loaded into a plastic vial and compressed into a dense pellet. The vial was then placed upside down in the equilibrium cell on top of a 5-cm layer of glass wool. The glass wool distributed the carbon dioxide entering the cell and ensured that it was not directed at the vial in a concentrated jet. The equilibrium cell was then pressurized and kept at 313 K and 15 MPa for at least 10 min. If the solid melted in the presence of the supercritical carbon dioxide, it came out of the vial. Pure lauric acid, myristic acid, LLL, and MMM as well as the mixtures LLL–MMM and LLL–MMM–PPP melted, while pure palmitic acid, PPP, and the mixtures LLL–PPP and MMM–PPP did not melt.

Materials. Palmitic acid (Sigma, 99–100% pure), myristic acid (Aldrich, 99.5% pure), lauric acid (Sigma, 99% pure), and LLL (Sigma, 99% pure) were used as received. PPP and MMM (both Sigma, 99% pure) were purified by SCF extraction prior to the experiments in order to remove impurities that are soluble in supercritical CO_2. Carbon dioxide (Colony, 99.92% pure) was used as received.

Modelling

Solubility data were modelled by a lattice model equation of state (EOS) that was developed to correlate equilibrium data from mixtures of molecules of disparate sizes (*22*, *23*). While we shall present a brief synopsis of the model here, a more detailed description has been presented elsewhere (*18*). In this model, molecules are assumed to occupy cells in a three-dimensional cubic lattice of coordination number z (set to 10) and of cell size v_H (set to 9.75×10^{-6} m^3 mol^{-1}). Each molecule (denoted by the subscript 1) is assumed to occupy r_1 sites, and the lattice has empty sites termed "holes" (denoted by a subscript 0). Under these assumptions the EOS that defines a *pure* component is

$$\frac{\tilde{P}}{\tilde{T}} = \ln\left(\frac{\tilde{v}}{\tilde{v}-1}\right) + \frac{z}{2}\ln\left(\frac{\tilde{v}+(q_1/r_1)-1}{\tilde{v}}\right) - \frac{\vartheta^2}{\tilde{T}} \quad (1)$$

where ϑ is the surface area fraction of sites in the lattice that are occupied by molecular segments. (zq_1) is the number of external contacts per molecule, P the pressure, T the temperature, and v the specific volume. The tilde ($\tilde{\ }$) denotes reduced variables, which are defined by the equations

$$\tilde{P} = P/P^*, \quad \tilde{T} = T/T^*, \quad \tilde{v} = v/v^* \quad (2a)$$

P^* and T^*, the quantities used in reducing P and T to nondimensional variables, are related by the equation

$$(z/2)\epsilon_{11} = P^* v_H = RT^* \quad (2b)$$

where ϵ_{11} is the interaction energy betweeen segments of molecules. In the EOS for each pure component, therefore, there are two unknown parameters, ϵ_{11} and v^*, the reducing parameter for volume.

Application of eq 1 requires determination of ϵ_{11} and v^*. For pure components below their critical points, the technique of Joffe et al. (*24*) was employed. This involved matching the chemical potentials of the component across the liquid and vapor phases at the vapor pressure of the substance.

$$\mu^L = \mu^V \quad (3a)$$

Also the actual and predicted saturated liquid densities were matched: matched:

$$v^L(\text{computed}) = v^L(\text{experiment}) \quad (3b)$$

Table I. Pure Component Model Parameters Used

compd	T, K	T_c, K	P_c, MPa	ϵ_{11}/R, K	v^*, $cm^3\ g^{-1}$
carbon dioxide[a]	310–370	304.2	7.38	82.03	0.82
lauric acid[b]	313			129.75	1.10
myristic acid[b]	313			128.45	1.11
palmitic acid[b]	313			127.07	1.12
triglycerides[c]	338			102.65	1.18

[a] P–v data for carbon dioxide from ref 25. [b] P–v data for fatty acids from ref 26. [c] P–v data for triglycerides estimated from ref 27.

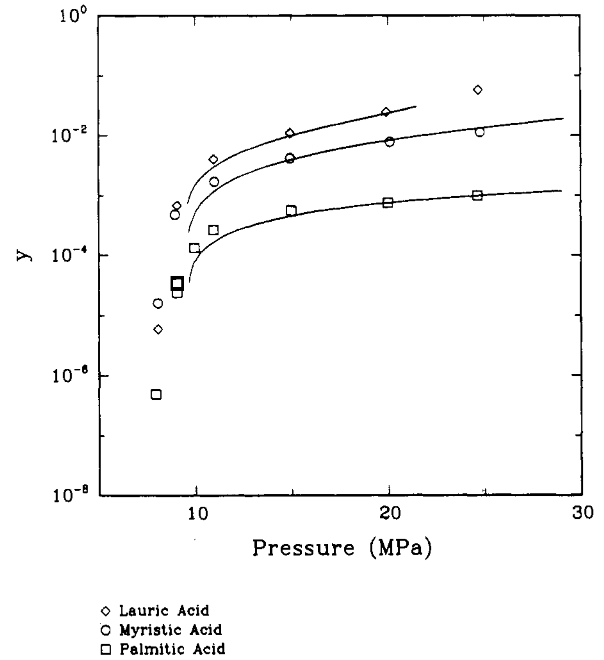

Figure 2. Solubility of pure fatty acids in CO_2. Points represent experimental data and curves are model predictions.

This set of equations was solved by the use of Newton's method to yield the pure component parameters listed in Table I. It was found that eq 3 could be solved with relative ease for the three fatty acids considered in this study. For the triglycerides however, due to the unusually small vapor pressures, it was possible to determine the pure component parameters only for trilaurin, which has the highest vapor pressure of the three triglycerides. Consistent with our earlier work (*18*, *22*, *23*), we assumed that ϵ_{11} and v^* were identical for all the three triglycerides considered.

For CO_2 which was above its critical point, the pure component parameters were obtained by fitting the EOS (eq 1) to isothermal P–v data (*25–27*). These parameters are listed in Table I.

Extension of this model to binary and multicomponent mixtures requires mixing and combining rules. The coordination number (z) and the lattice size (v_H) are assumed constant, independent of composition. A linear mixing rule of the type

$$B_M = \sum B_i y_i \tag{4}$$

is used for the mixture parameters v^*, q, and r. In eq 4, B represents some generalized property, while y_i is the *mole fraction* of component i in the relevant phase. The mixing rule for the energy parameter (ϵ_{11}) is (*23*)

$$\epsilon_M = \sum\sum \vartheta_i \vartheta_j \epsilon_{ij} \Gamma_{ij} \tag{5}$$

where ϑ_i is the surface area fraction of the segments of i molecules and Γ_{ij} is a factor that corrects for the nonrandom distribution of segments of j molecules about the segments of i molecules. (This factor is obtained by the solution of the quasi-chemical equations. See ref *22* for more details.) The combining rule for the mixture parameter ϵ_{ij} in eq 5 is

$$\epsilon_{ij} = \epsilon_{ii} \qquad (i = j)$$

$$\epsilon_{ij} = \tfrac{1}{2}(\epsilon_{ii} + \epsilon_{jj})(1 - \delta_{ij}) \qquad (i \neq j) \tag{6}$$

where δ_{ij} represents a single adjustable parameter (per binary) used in fitting the model to data.

Table II. Solubilities of Pure Lauric Acid in Carbon Dioxide

press., MPa	reduced density	mole fraction	press., MPa	reduced density	mole fraction
7.7	0.5	4.13×10^{-7}	15.0	1.7	1.10×10^{-2}
8.1	0.6	2.36×10^{-5}	15.0	1.7	1.08×10^{-2}
8.1	0.6	5.95×10^{-6}	15.1	1.7	1.11×10^{-2}
9.1	1.0	6.78×10^{-4}	20.0	1.8	2.48×10^{-2}
11.0	1.5	4.06×10^{-3}	24.8	1.9	5.73×10^{-2}

Table III. Solubilities of Pure Myristic Acid in Carbon Dioxide

press., MPa	reduced density	mole fraction	press., MPa	reduced density	mole fraction
8.2	0.6	1.61×10^{-5}	15.0	1.7	4.21×10^{-3}
9.0	1.0	4.81×10^{-4}	20.2	1.8	7.81×10^{-3}
11.1	1.5	1.70×10^{-3}	24.9	1.9	1.13×10^{-2}
15.0	1.7	4.14×10^{-3}			

Table IV. Solubilities of Pure Palmitic Acid in Carbon Dioxide

press., MPa	reduced density	mole fraction	press., MPa	reduced density	mole fraction
8.0	0.6	4.96×10^{-7}	15.1	1.7	5.54×10^{-4}
9.1	1.0	2.42×10^{-5}	15.1	1.7	5.62×10^{-4}
9.1	1.0	3.48×10^{-5}	20.1	1.8	7.59×10^{-4}
10.0	1.3	1.33×10^{-4}	24.8	1.9	9.95×10^{-4}
11.0	1.5	2.67×10^{-4}			

Table V. Model Interaction Parameters

compd	δ_{ij}	compd	δ_{ij}
lauric acid	0.06	trilaurin	0.09
myristic acid	0.07	trimyristin	0.105
palmitic acid	0.12	tripalmitin	0.13

Results and Discussion

Solubility of Pure Fatty Acids in Supercritical CO_2. In Figure 2 we present a plot of the experimental solubility (denoted by points) of the three fatty acids in supercritical CO_2 at 313 K. The same data are also tabulated in Tables II, III, and IV. The isotherms for each compound, as expected, show rapid increases in solubility in the vicinity of the critical density of CO_2 (corresponding to a pressure of approximately 9.5 MPa at 313 K). Also, the increase in solubility with pressure for all compounds except lauric acid is much lower at pressures in excess of ca. 15 MPa. The solubility isotherm of lauric acid, however, is still increasing at the highest pressure at which it was measured, i.e., at 25 MPa. This implies that the lauric acid–carbon dioxide binary may be close to its upper critical end point (UCEP) temperature under these conditions.

Data for the solubility of the three fatty acids in CO_2 were correlated with the lattice model EOS along with the appropriate pure component parameters that have been presented earlier (Table I). Since the lauric acid–CO_2 mixture may be close to its UCEP, substantial quantities of the SCF should be dissolved in the solid lauric acid phase. In contrast to earlier practice (*20*) therefore, we chose not to model the condensed phases for all three systems as pure; instead, the lattice EOS was employed as the appropriate thermodynamic model for both phases. Results obtained from the correlation are shown as solid lines in Figure 2. A single adjustable parameter, δ_{ij}, is required to fit the model satisfactorily to each binary. The

Table VI. Solubilities of Pure Trilaurin in Carbon Dioxide

press., MPa	reduced density	mole fraction	press., MPa	reduced density	mole fraction
9.1	1.1	1.32×10^{-5}	15.1	1.7	9.02×10^{-4}
11.1	1.5	2.28×10^{-4}	20.0	1.8	1.83×10^{-3}
15.1	1.7	8.74×10^{-4}	25.3	1.9	3.37×10^{-3}

Table VII. Solubilities of Pure Trimyristin in Carbon Dioxide

press., MPa	reduced density	mole fraction	press., MPa	reduced density	mole fraction
9.5	1.2	1.23×10^{-5}	15.4	1.7	2.00×10^{-4}
11.1	1.5	5.55×10^{-5}	20.2	1.8	3.43×10^{-4}
15.2	1.7	1.92×10^{-4}	24.9	1.9	4.22×10^{-4}
15.3	1.7	2.15×10^{-4}	30.4	1.9	4.95×10^{-4}

Table VIII. Solubilities of Pure Tripalmitin in Carbon Dioxide

press., MPa	reduced density	mole fraction	press., MPa	reduced density	mole fraction
12.2	1.5	3.03×10^{-6}	19.8	1.8	1.50×10^{-5}
15.0	1.7	6.71×10^{-6}	24.8	1.9	2.39×10^{-5}
15.0	1.7	6.81×10^{-6}	29.7	1.9	2.71×10^{-5}
15.0	1.7	6.95×10^{-6}			

values of this parameter for each system are listed in Table V. The δ_{ij} values for the three acid systems follow a consistent trend: increasing with increasing molecular weight of the solute in consideration.

An interesting aspect of the modelling results is that although the predictions of the lattice EOS for the lauric acid–CO_2 system agree with the experimental results up to 22 MPa, beyond this pressure the model predicts that the solute is completely miscible in the SCF. Although this result is inconsistent with our measurements for this binary at higher pressure, this nevertheless lends credence to the deduction that this binary mixture is close to its UCEP. The incorrect prediction of the lattice model for the UCEP pressure is not surprising, since the EOS, having been derived through the use of a mean-field theory, cannot be utilized to accurately model phase behavior in the vicinity of critical points. For the same reason, the model does not accurately describe the behavior of the system near the critical point of the solvent. Therefore, model results are not shown for pressures below about 9.6 MPa.

Solubility of Pure Triglycerides in Supercritical CO_2. The solubilities of the pure triglycerides are presented in Tables VI, VII, and VIII and also as data points in Figure 3. The fits to the experimental data with the lattice model are also shown and these are represented in Figure 3 by smooth curves. Trends observed with the triglycerides closely match the results obtained with myristic acid and palmitic acid. The solubilities of the triglycerides increase steeply with pressure near 9.5 MPa and then more slowly at higher pressures.

The solubility of PPP was measured by Chrastil (*5*) in a batch system. The values that he obtained were about an order of magnitude higher than ours. We speculate that any highly soluble impurities present in the PPP could have possibly resulted in artifically enhanced measurements of solubility. In our own experiments using PPP of lower quality (90%) than that used for our other experiments (99%), we measured solubilities that were even higher than Chrastil's. This demonstrates the sensitivity of solubility measurements to the purity of the material being used.

It is interesting to note that the solubilities of LLL and palmitic acid are about the same, although they differ in molecular weight by a factor of ~2.5. We propose that this may be due to the fact that the fatty acid has a polar carboxylic acid group, making it less soluble in CO_2, while the triglyceride, being relatively nonpolar, is more soluble. This type of effect has been reported for organic compounds of lower molecular weight (*19*).

Table IX. Solubilities of the Mixture Trilaurin–Trimyristin in Carbon Dioxide

press., MPa	reduced density	mole fraction	
		trilaurin	trimyristin
9.2	1.1	1.86×10^{-5}	1.84×10^{-6}
11.0	1.5	1.44×10^{-4}	2.99×10^{-5}
15.1	1.7	5.81×10^{-4}	1.16×10^{-4}
15.2	1.7	5.60×10^{-4}	1.13×10^{-4}
15.2	1.7	5.67×10^{-4}	1.31×10^{-4}
15.2	1.7	5.72×10^{-4}	1.36×10^{-4}
19.9	1.8	1.11×10^{-3}	3.11×10^{-4}
24.9	1.9	1.89×10^{-3}	4.86×10^{-4}

Table X. Solubilities of the Mixture Trilaurin–Tripalmitin in Carbon Dioxide

press., MPa	reduced density	mole fraction	
		trilaurin	tripalmitin
9.1	1.1	1.28×10^{-5}	4.50×10^{-8}
11.1	1.5	2.18×10^{-4}	5.24×10^{-7}
15.2	1.7	8.68×10^{-4}	6.09×10^{-6}
15.3	1.7	8.59×10^{-4}	6.26×10^{-6}
20.0	1.8	1.66×10^{-3}	2.43×10^{-5}
24.7	1.9	2.83×10^{-3}	6.20×10^{-5}

Table XI. Solubilities of the Mixture Trimyristin–Tripalmitin in Carbon Dioxide

press., MPa	reduced density	mole fraction	
		trimyristin	tripalmitin
9.2	1.1	5.02×10^{-6}	3.53×10^{-7}
11.0	1.5	5.50×10^{-5}	3.20×10^{-6}
15.1	1.7	1.29×10^{-4}	1.13×10^{-5}
15.2	1.7	1.31×10^{-4}	1.13×10^{-5}
15.3	1.7	1.35×10^{-4}	1.05×10^{-5}
20.0	1.8	2.84×10^{-4}	2.69×10^{-5}
25.0	1.9	4.07×10^{-4}	3.22×10^{-5}
30.4	1.9	4.83×10^{-4}	3.85×10^{-5}

Table XII. Solubilities of the Mixture Trilaurin–Trimyristin–Tripalmitin in Carbon Dioxide

press., MPa	reduced density	mole fraction		
		trilaurin	trimyristin	tripalmitin
9.2	1.1	1.71×10^{-5}	3.98×10^{-6}	1.98×10^{-7}
11.1	1.5	1.49×10^{-4}	4.12×10^{-5}	2.78×10^{-6}
15.0	1.7	4.62×10^{-4}	1.41×10^{-4}	1.03×10^{-5}
15.0	1.7	4.76×10^{-4}	1.31×10^{-4}	1.04×10^{-5}
15.1	1.7	6.63×10^{-4}	8.74×10^{-5}	1.11×10^{-5}
15.1	1.7	6.08×10^{-4}	7.75×10^{-5}	9.53×10^{-6}
15.3	1.7	5.28×10^{-4}	1.36×10^{-4}	1.19×10^{-5}
19.9	1.8	9.02×10^{-4}	3.25×10^{-4}	3.55×10^{-5}
25.0	1.9	1.62×10^{-3}	5.07×10^{-4}	4.75×10^{-5}

The lattice model was found to correlate the data effectively using the δ_{ij} values shown in Table V. The deviations at low pressure (near the critical point of the solvent) are due to the inability of the model to predict thermodynamic properties near critical points, as discussed in the previous section. As with the fatty acids, the model could not be used for pressures below about 9.6 MPa. The δ_{ij}'s increase almost linearly with molecular weight, providing us with a technique to estimate approximate solubilities of other triglycerides that might not be available as pure substances.

Solubilities of Triglyceride Mixtures in CO_2. There are four different mixtures that may be formed with the three triglycerides and CO_2. There are three ternary systems with two triglycerides and CO_2, and one quaternary system with all three triglycerides plus CO_2. Solubilities in all four systems were measured in this work and are presented in Tables IX, X, XI, and XII and in Figures 4–7. In Figures 4–7, the open symbols are for binary systems (presented in Figure 3 and Tables VI, VII, and VIII) and the closed symbols represent the solubilities of the corresponding compounds in the ternary or quaternary

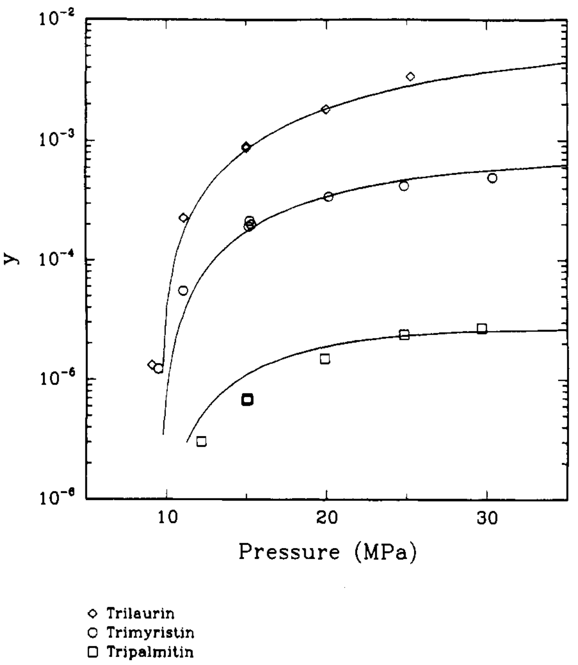

Figure 3. Solubility of pure triglycerides in CO_2. Points represent experimental data and curves are model predictions.

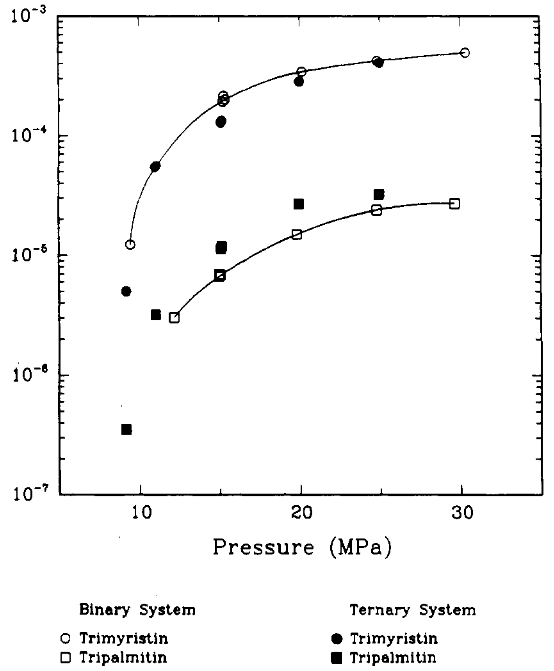

Figure 4. Solubility of the ternary mixture MMM-PPP in CO_2. Open symbols represent binary data (presented in Figure 3) and closed symbols represent mixture data. Lines are cubic fits of binary data and are included to make the graph easier to read.

mixtures. The solid lines are a cubic fit of the binary data and are included to make the graphs easier to read. Although a multicomponent lattice EOS has been developed, we have not, as yet, implemented it. Therefore, none of the ternaries nor the quaternary were modeled with the lattice EOS.

Data for the ternary systems PPP-MMM-CO_2 and PPP-LLL-CO_2 are presented in Figures 4 and 5. Since the triglyceride-rich phase in these systems was shown to be solid under extraction conditions, we assume that interactions between different types of triglycerides in the solid phase do not affect the individual solubility of a compound in CO_2. We found that when the relative amounts of triglycerides charged to the cell in these mixtures were changed by about 20%, the solubility of each species in the supercritical phase did not change. Interactions in the supercritical phase, however, are relevant. It is therefore appropriate to use the mole fraction of the component in the supercritical phase as the correlating variable.

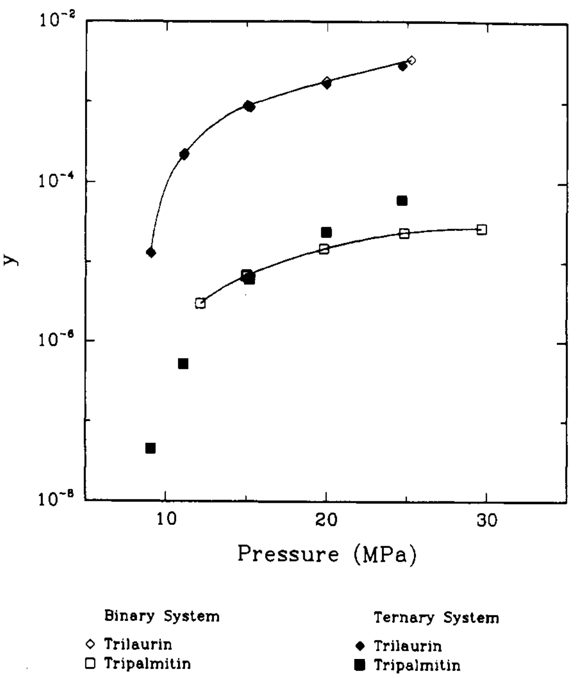

Figure 5. Solubility of the ternary mixture LLL-PPP in CO_2. Open symbols represent binary data (presented in Figure 3) and closed symbols represent mixture data. Lines are cubic fits of binary data and are included to make the graph easier to read.

The solubility of the lighter compound (MMM or LLL) was not greatly affected by the presence of the heavier compound, while the solubility of the heavier compound (PPP) was enhanced by the presence of the lighter one. It is not surprising that the solubility of the MMM or LLL was not affected by the presence of PPP because the PPP concentration was at least an order of magnitude lower than that of MMM or LLL. By the same token, the increase in solubility of the PPP may be explained by invoking the fact that the other triglyceride (LLL or MMM) which is present in much higher concentration than PPP, acts as an entrainer, enhancing the PPP solubility. This type of solubility enhancement has been observed by others (*4*, *28*, *29*).

The system MMM-LLL-CO_2 was shown to melt under the extraction conditions. Thus, intermolecular interactions in the liquid phase are expected to affect the solubilities in the supercritical phase. Indeed, different mole fractions of triglyceride charged to the cell gave different solubilities. For this reason, the correlating variable was chosen to be the partition coefficient K_i, defined as

$$K_i = y_i/x_i \tag{7}$$

where y_i is the measured mole fraction of component i in the supercritical phase and x_i is the calculated mole fraction of component i in the liquid phase neglecting the concentration of CO_2 dissolved in the liquid. The solubility data for this mixture are represented by K_i, as shown in Table XIII and Figure 6. In Figure 6, the open symbols represent the binary data presented earlier. For the binaries, $x_i = 1$, so $K_i = y_i$. The solid line is a cubic fit of the binary data and the filled symbols represent the ternary mixture data. All the data points for a given compound fall along the same line, regardless of the liquid-phase composition when K is used as the correlating variable. This is not the case for data correlated with y_i.

The trend is the same as that observed in the other ternary systems. The partition coefficient of the most soluble compo-

Table XIII. Partition Coefficients for Trilaurin (2)–Trimyristin (3) in Carbon Dioxide

press., MPa	y_2	y_3	x_2	x_3	K_2	K_3
9.3	1.86×10^{-5}	1.84×10^{-6}	0.603	0.397	3.08×10^{-5}	4.63×10^{-5}
11.0	1.44×10^{-4}	2.99×10^{-5}	0.600	0.400	2.40×10^{-4}	7.48×10^{-5}
15.1	5.81×10^{-4}	1.16×10^{-4}	0.568	0.432	1.02×10^{-3}	2.68×10^{-4}
15.2	5.67×10^{-4}	1.31×10^{-4}	0.505	0.495	1.12×10^{-3}	2.65×10^{-4}
15.2	5.60×10^{-4}	1.13×10^{-4}	0.606	0.394	9.24×10^{-4}	2.87×10^{-4}
19.9	1.11×10^{-3}	3.11×10^{-4}	0.594	0.406	1.88×10^{-3}	7.65×10^{-4}
24.8	1.89×10^{-3}	4.86×10^{-4}	0.580	0.420	3.26×10^{-3}	1.16×10^{-3}

Table XIV. Partition Coefficients for Trilaurin (2)–Trimyristin (3)–Tripalmitin (4) in Carbon Dioxide

press., MPa	y_2	y_3	y_4	x_2	x_3	x_4	K_2	K_3	K_4
9.2	1.71×10^{-5}	3.98×10^{-6}	1.98×10^{-7}	0.462	0.319	0.219	3.71×10^{-5}	1.25×10^{-5}	9.03×10^{-7}
11.1	1.49×10^{-4}	4.12×10^{-5}	2.78×10^{-6}	0.459	0.321	0.220	3.25×10^{-4}	1.28×10^{-4}	1.26×10^{-5}
15.0	4.76×10^{-4}	1.31×10^{-4}	1.04×10^{-5}	0.438	0.327	0.235	1.09×10^{-3}	4.01×10^{-4}	5.31×10^{-5}
15.0	4.62×10^{-4}	1.41×10^{-4}	1.03×10^{-5}	0.464	0.319	0.217	9.97×10^{-4}	4.42×10^{-4}	4.73×10^{-5}
15.1	6.63×10^{-4}	8.74×10^{-5}	1.11×10^{-5}	0.624	0.206	0.170	1.06×10^{-3}	4.24×10^{-4}	6.50×10^{-5}
15.1	6.08×10^{-4}	7.75×10^{-5}	9.53×10^{-6}	0.618	0.208	0.174	9.84×10^{-4}	3.73×10^{-4}	5.48×10^{-5}
15.2	5.28×10^{-4}	1.36×10^{-4}	1.19×10^{-5}	0.469	0.316	0.215	1.13×10^{-3}	4.29×10^{-4}	5.53×10^{-5}
19.9	9.02×10^{-4}	3.25×10^{-4}	3.55×10^{-5}	0.455	0.321	0.224	1.98×10^{-3}	1.01×10^{-3}	1.58×10^{-4}
2.5	1.62×10^{-3}	5.07×10^{-4}	4.75×10^{-5}	0.446	0.324	0.230	3.63×10^{-3}	1.57×10^{-3}	2.06×10^{-4}

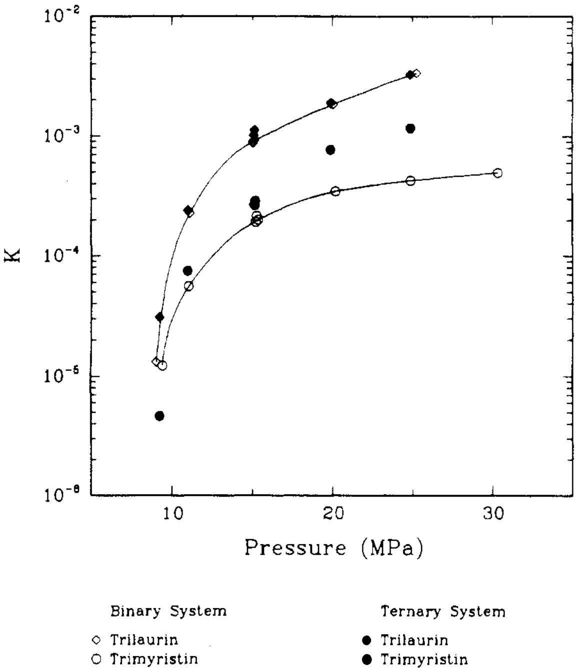

Figure 6. Solubility of the ternary mixture LLL–MMM in CO_2. Open symbols represent binary data (presented in Figure 3) and closed symbols represent mixture data. Lines are cubic fits of binary data and are included to make the graph easier to read.

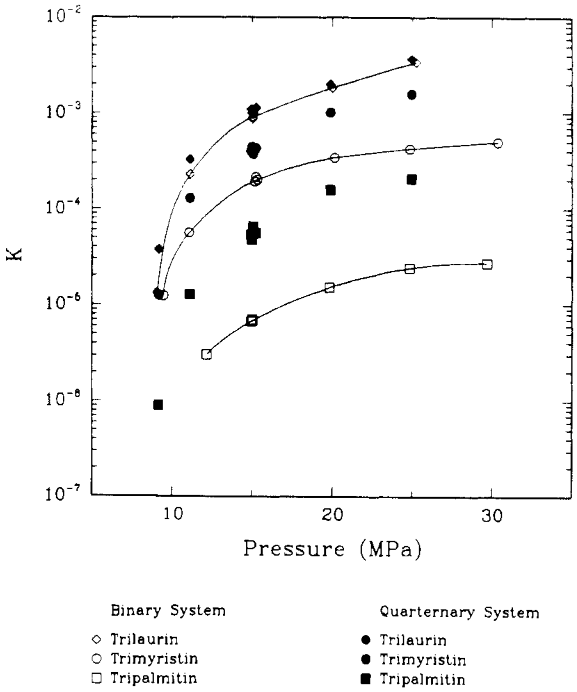

Figure 7. Solubility of the quaternary mixture LLL–MMM–PPP in CO_2. Open symbols represent binary data (presented in Figure 3) and closed symbols represent mixture data. Lines are cubic fits of binary data and are included to make the graph easier to read.

nent (LLL) is unchanged while that of the less soluble compound (MMM) is enhanced compared to the binary systems.

The data for the quaternary system PPP–MMM–LLL–CO_2 are presented in Table XIV and Figure 7. Open symbols are for binary data and lines are cubic fits of the binary data. Filled symbols are for the quaternary mixture. Since this mixture also melts under the extraction conditions, the partition coefficient *K* was used as the correlating variable. Here again, the most soluble compound (LLL) has the same partition coefficient as it does in the binary system while the less soluble compounds (PPP and MMM) have higher partition coefficients in the mixture than in the binaries. The solubility enhancement is stronger in the quaternary system than in the ternary systems.

Conclusions

Solubilities in CO_2 of three pure fatty acids and three pure triglycerides were measured and these binary data were correlated by using a lattice model EOS. The EOS accurately predicts solubilities outside the critical region. Solubilities of triglyceride mixtures were also measured. The solubility of the most soluble compound was the same as the binary solubility, but the solubility of the less soluble component was enhanced. This is most likely due to an entrainer effect caused by the more soluble compound. For the mixtures which melted under the conditions at which the solubility measurements were carried out, the mole fraction of the different triglycerides in the supercritical fluid phase varied as the composition of the liquid phase changed, implying that intermolecular interactions in the liquid phase affect solubility in the supercritical phase. The supercritical fluid phase solubility could, however, be correlated with the use of a partition coefficient calculated as the ratio of mole fraction of a particular triglyceride in the supercritical phase to the mole fraction of that compound in the liquid phase on a CO_2-free basis. This implies that dissolved CO_2 in the liquid phase does not affect solubilities of triglycerides in the supercritical phase.

In order to model the CO_2 solubilities of triglyceride mixtures, it is necessary to take into account intermolecular interactions between unlike triglycerides in both the supercritical and liquid (or solid) phases. Research is underway to use a multicomponent version of the lattice EOS to correlate solubility data of mixtures by using pure component parameters and binary interactions parameters δ_{ij}, from independent measurements, along with a fitted interaction parameter that would take into account interactions between unlike solute species.

Glossary

K	partition coefficient
P	pressure
q	effective chain length of a chain molecule
R	gas constant
r	number of segments per molecule
T	absolute temperature
v	specific volume
v_H	lattice unit cell volume
x	mole fraction, in particular in the heavy phase
y	mole fraction in the light phase
z	lattice cell coordination number

Greek Letters

δ_{ij}	binary interaction parameter in EOS
ϵ_{ij}	interaction energy between molecule segments
Γ	nonrandomness correction
μ	chemical potential
ϑ	molecular surface area fraction

Superscripts

•	reducing quantity
~	reduced quantity
L	liquid phase
V	vapor phase

Subscripts

i	species i
j	species j
M	mixture property

Acknowledgment

We thank Professor Bob Reid for very helpful discussions.

Registry No. LLL, 538-24-9; MMM, 555-45-3; PPP, 555-44-2; CO_2, 124-38-9; lauric acid, 143-07-7; myristic acid, 544-63-8; palmitic acid, 57-10-3.

Literature Cited

(1) McHugh, M. A.; Krukonis, V. J. *Supercritical Fluid Extraction: Principles and Practice*; Butterworths: Boston, 1986.
(2) Friedrich, J.; Pryde, E. *J. Am. Oil Chem. Soc.* **1984**, *61*, 223-228.
(3) Brannolte, H.; Mangold, H.; Stahl, E. *Chem. Phys. Lipids* **1983**, *33*, 297-299.
(4) Brunner, G.; Peter, S. *Sep. Sci. Tech.* **1982**, *17*, 199-214.
(5) Chrastil, J. *J. Phys. Chem.* **1982**, *86*, 3016-3021.
(6) Christianson, D.; Friedrich, J.; List, G.; Warner, K.; Bagley, E.; Stringfellow, A.; Inglett, G. *J. Food Sci.* **1984**, *49*, 229-232.
(7) Eisenbach, W. *Ber. Bunsenges. Phys. Chem.* **1984**, *88*, 882-887.
(8) Friedrich, J.; List, G.; Heakin, A. *J. Am. Oil Chem. Soc.* **1982**, *59*, 288-292.
(9) List, G.; Friedrich, J.; Christianson, D. *J. Am. Oil Chem. Soc.* **1984**, *61*, 1849-1851.
(10) List, G.; Friedrich, J.; Pominski, J. *J. Am. Oil Chem. Soc.* **1984**, *61*, 1847-1849.
(11) Snyder, J.; Friedrich, J.; Christianson, D. *J. Am. Oil Chem. Soc.* **1984**, *61*, 1851-1856.
(12) Stahl, E.; Quirin, K.; Glatz, A.; Gerard, D.; Rau, G. *Ber. Bunsenges. Phys. Chem.* **1984**, *88*, 900-907.
(13) Stahl, E.; Quirn, K.; Mangold, H. *Chem. Phys. Lipids* **1982**, *31*, 319-324.
(14) Stahl, E.; Schilz, W. *Chem. Ing. Tech.* **1976**, *48*, 773-778.
(15) Stahl, E.; Schilz, W.; Schütz, E.; Willing, E. *Angew. Chem., Int. Ed. Engl.* **1978**, *17*, 731-738.
(16) Passino, H. *Ind. Eng. Chem.* **1949**, *41*, 280-287.
(17) Dickinson, N.; Meyers, J. *J. Am. Oil Chem. Soc.* **1959**, *29*, 235-239.
(18) Kumar, S. Sc.D. Thesis, Massachusetts Institute of Technology, Cambridge, MA, 1986.
(19) Schmitt, W. Ph.D. Thesis, Massachusetts Institute of Technology, Cambridge, MA, 1984.
(20) Kurnik, R.; Holla, S.; Reid, R. *J. Chem. Eng. Data* **1981**, *26*, 47-51.
(21) Tsekhanskaya, Y.; Iomtev, M.; Mushkina, E. *Russ. J. Phys. Chem.* **1964**, *38*, 1173.
(22) Kumar, S.; Reid, R.; Suter, U. *ACS Div. Fuel Chem. Prepr.* **1985**, *30*, 66-77.
(23) Kumar, S.; Suter, U.; Reid, R. *Ind. Eng. Chem.* **1987**, *26*, 25-32.
(24) Joffe, J.; Schroeder, G.; Zudgevitch, D. *AIChE J.* **1970**, *49*, 419.
(25) Angus, S.; Armstrong, B.; de Reuck, K. *International Thermodynamic Tables of the Fluid State of Carbon Dioxide*; Permagon: Oxford, U.K., 1976.
(26) *The Merck Index*, 10th ed.; Merck: Rahway, NJ, 1983.
(27) Bailey, A. *Bailey's Industrial Oil and Fat Products*, 4th ed.; Wiley: New York, 1979.
(28) van Gunst, Ph.D. Dissertation, University of Delft, 1950.
(29) Kurnik, R.; Reid, R. *Fluid Phase Equilib.* **1982**, *8*, 93.

Received for review August 17, 1987. Accepted February 25, 1988. T.B. thanks the Ernest Solvay Foundation for financial support during his stay at MIT. J.C.E. was supported in part by a Pfizer Fellowship in Biochemical Engineering. S.K.K. thanks Professor Ulrich Suter for financial support during the course of this work.

Enthalpies of Mixing of Diethyl Sulfide + Carbon Tetrachloride and Diethyl Sulfide + Chloroform at 25 °C

Donald F. Gray, Neil F. Pasco, and Arthur G. Williamson*

Department of Chemical and Process Engineering, University of Canterbury, Christchurch, New Zealand

Enthalpies of mixing of mixtures of diethyl sulfide with carbon tetrachloride and with chloroform at 298.15 K are reported. The diethyl sulfide mixtures are more exothermic than the corresponding dimethyl sulfide mixtures measured earlier by Gray and Williamson by about 300 J mol^{-1}.

Introduction

The measurements reported here are part of a continuing study of solutions of ether and thioether mixtures with chlorinated hydrocarbons being carried out in this laboratory in which both weak and strong specific interactions are observed.

Experimental Section

The calorimeter used in this work is of the type originally developed by McGlashan and his colleagues (*2*) and has been fully described elsewhere (*3*). The measurements from this calorimeter are expected to be accurate to ±1-2% for exothermic systems.

Materials

Carbon tetrachloride and chloroform were purified as described by Beath and Williamson (*3*). The alkyl sulfides were

0021-9568/88/1733-0333$01.50/0 © 1988 American Chemical Society